Biomaterials Science

ROYAL SOCIETY OF CHEMISTRY

PAPER

View Article Online
View Journal | View Issue

Cite this: *Biomater. Sci.*, 2025, **13**, 6169

Investigating PolySTAT's role in clot contraction and fibrin network mechanics

Trey J. Pichon,†[a,b,c] Trevor Corrigan, †[a,b,c] Melissa Ling,[b] Mishti Dhawan,[a,b] Anna Tobiasch,[e] Mirjam Bachler,[e] Martin Hermann,[e] Dietmar Fries,[e] Matthew Armstrong,[f] Suzie H. Pun *[a,b,c] and Nathan J. White*[a,c,d]

PolySTAT is a synthetic polymer-based hemostat that binds to and physically crosslinks fibrin, the primary structural component of blood clots. By modifying fibrin architecture and enhancing resistance to fibrinolysis, PolySTAT increased survival rates rat models of severe hemorrhage. Recently, we observed that clots treated with PolySTAT contracted at a higher rate than untreated controls. Clot contraction, driven by platelet activity, is known to contribute to clot stabilization and reduction of blood loss by promoting wound closure. This work explores PolySTAT's influence beyond its antifibrinolytic function, with emphasis on platelet-driven clot contraction. We demonstrate that PolySTAT enhances clot contraction in human blood by altering the fibrin network rather than directly modulating platelet activity. Using direct measurements of clot contraction forces in human whole blood, we observed that PolySTAT increased both the rate and magnitude of platelet-generated forces. To assess the mechanical consequences of these microstructural changes, rheological testing was performed across both linear and nonlinear viscoelastic regimes. The data indicate that PolySTAT increases the elastic modulus of clots, providing a stiffer substrate for platelet engagement, and strengthens the fibrin network against mechanical failure while enabling recovery after deformation. Based on these findings, we propose that clots formed in the presence of PolySTAT transmit platelet forces through the fibrin matrix with greater efficiency, which may accelerate clot contraction and contribute to improved hemostatic function.

Received 21st July 2025,
Accepted 23rd September 2025

DOI: 10.1039/d5bm01101a

rsc.li/biomaterials-science

1. Introduction

Trauma is the leading cause of death worldwide for young adults, accounting for over 4 million deaths annually in 2019.[1–3] Uncontrolled bleeding is the primary cause of preventable death in trauma.[4,5] The "triad of death", a combination of coagulopathy with hypothermia and acidosis, increases mortality in trauma patients and early intervention is critical to survival.[6] Damage Control Resuscitation (DCR) emerged during the last several decades as a critical lifesaving mechanism capable of combating the triad of death. Hemostatic resuscitation is a pillar of DCR that prevents coagulopathy typically accomplished using a solution as similar as possible to whole blood.[7] Blood transfusions are supplemented with the antifibrinolytic drug tranexamic acid (TXA).[8] Our group has developed an intravenous polymeric hemostat or PolySTAT, that consists of fibrin-binding peptides conjugated to a water-soluble polymer backbone. PolySTAT promotes hemostasis by selectively binding and physically crosslinking fibrin during clot formation at wounds. In preclinical models, PolySTAT increased survival and reduced bleeding.[9,10] We have previously shown that PolySTAT increases clot storage modulus by increasing fibrin fibril density and diameter leading to a denser fibrin network that is also resistant to fibrinolysis.[11] PolySTAT also appeared to enhance clot contraction *in vitro* in whole blood. This observation suggested that PolySTAT may influence platelet activity or platelet-induced clot contraction through integrin-mediated mechanotransduction and actomyosin signaling.[12,13] Building on our previous findings on fibrin density and fibrinolysis resistance, we investigated the effects of PolySTAT on platelets, clot contraction, and mechanical clot function. We hypothesized that PolySTAT increases the rate of clot contraction by more efficient distribution of platelet contractile forces through

[a]*Department of Bioengineering, University of Washington, 3720 15th Ave NE, Seattle, Washington 98195, USA. E-mail: spun@uw.edu, whiten4@uw.edu*
[b]*Molecular Engineering and Sciences Institute, University of Washington 3946 W Stevens Way NE, Seattle, Washington 98195, USA*
[c]*Resuscitation Engineering Science Unit (RESCU), University of Washington Harborview Research and Training Building, Seattle, Washington 98104, USA*
[d]*Department of Emergency Medicine, University of Washington, Seattle, Washington 98195, USA*
[e]*Department of Anaesthesia and Critical Care Medicine, Medical University of Innsbruck, Innsbruck, Austria*
[f]*Department of Chemical and Biomolecular Engineering, University of Delaware, Delaware, Maryland 19716, USA*
†These authors contributed equally.

mechanical transduction and clot stiffening. Our results showed that PolySTAT increased fibrin stiffness, improved the mechanical transduction efficiency of the fibrin network, and thereby accelerated clot contraction. These effects occurred independently of direct platelet activation.

2. Results and discussion

Rotational thromboelastometry (ROTEM) suggests PolySTAT increases platelet-induced clot contraction of rat and swine whole blood

PolySTAT (5 μM) decreased clot amplitude over time in rat whole blood by ROTEM indicating clot softening. This was contrary to previous findings of clot stiffening when using platelet-free plasmas and purified fibrin systems (Fig. 1A).[9–11] Furthermore, the addition of the antifibrinolytic aprotinin did not restore clot amplitude, suggesting a primary role for platelet-induced clot contraction away from the walls of the assay chamber rather than acute fibrinolysis. Clot retraction is a phenomenon that is well-documented in ROTEM and can be mistaken for clot lysis.[14–16]

To confirm clot contraction was occurring, the same blood samples were centrifuged to remove platelets, and the platelet-poor plasma was run again in both extrinsic (EXTEM) and aprotinin-containing (APTEM) thromboelastometry (Fig. 1B). In the absence of platelets, there were no differences in fibrin clot formation between conditions. Visual inspection of the center pins removed from the ROTEM cups revealed that PolySTAT treated clots had firmer, smaller clots retracted against the pin compared to the saline controls (Fig. S1). Samples of blood were then mixed with PolySTAT following the same protocol for EXTEM analysis except the samples were clotted in clear Eppendorf tubes for easy visualization (Fig. 1C). We observed more rapid clot contraction in all PolySTAT-treated blood samples compared to blood mixed with the saline volume control and observed comparable results in swine blood (Fig. S2).

PolySTAT and PolySCRAM bind to but do not directly activate platelets

To investigate if PolySTAT directly activates platelets we incubated PolySTAT and PolySCRAM (nonbinding negative control) with washed platelets (PAC-1 and P-selectin negative) from human donors (5 μM concentration, n = 3 donors, evaluated within 30 minutes of collection). ADP coincubation as a positive control showed strong platelet activation (Fig. 1D), while PolySTAT and PolySCRAM did not show any statistically signifi-

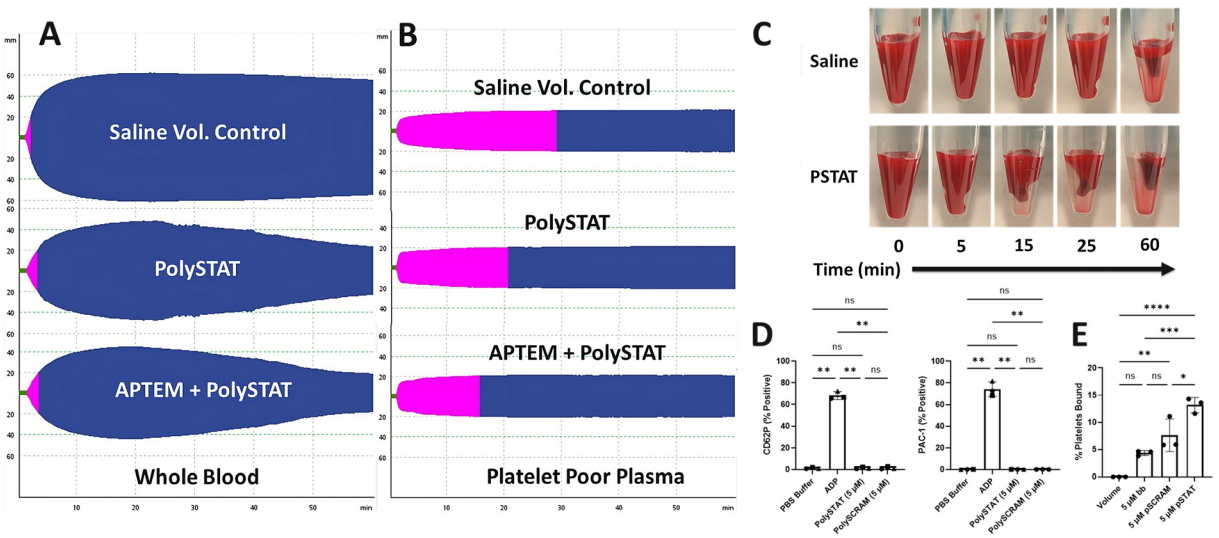

Fig. 1 PolySTAT increases clot contraction in swine, rats, and human whole blood PolySTAT increases clot contraction in swine, rats, and human whole blood. (A) Temograms of rat whole blood run in EXTEM assay with the saline volume control (top), PolySTAT dosed at 5 μM (middle), and 5 μM PolySTAT evaluated in the APTEM assay with the antifibrinolytic aprotinin (bottom). APTEM was unable to prevent the reduction in observed clot strength, confirming this to be a contraction-related ROTEM pattern rather than clot lysis. (B) The same rat whole blood samples were spun down to remove platelets, and plasma was evaluated in EXTEM with saline volume control (top), PolySTAT dosed at 5 μM (middle), and 5 μM PolySTAT evaluated in the APTEM assay with the antifibrinolytic aprotinin (bottom). No lysis was observed indicating that platelets were responsible for the contraction-related ROTEM pattern. (C) Qualitative comparison of the extent of clot contraction of swine whole blood clotted using the EXTEM reagents from ROTEM in 1.5 mL Eppendorf tubes. Compared to the saline volume control, PolySTAT at 5 μM increased the rate of clot contraction, and treated clots contracted to smaller volumes and a greater amount of erythrocyte sedimentation was observed. (D) PolySTAT does not activate platelets *via* flow cytometry (n = 3 human donors). Washed platelets from n = 3 human donors were evaluated for platelet activation *via* CD62P (P-selectin, left) and PAC-1 (right) after being incubated with PolySTAT and PolySCRAM at 5 μM concentration in whole blood. ADP and PBS were used as the positive control and negative volume control, respectively. (E) PolySTAT binds to washed human platelets (n = 3 human donors). FITC-labeled PolySTAT, PolySCRAM, and polymer backbone "GmMA" were incubated with washed platelets at 5 μM and compared to a PBS negative volume control. A fit model for a repeated measure, one-way Anova with Tukey *post-hoc* analysis (α = 0.050) was used to compare treatments. The following significance labels were used: ns ($P > 0.05$), * ($P \leq 0.05$), ** ($P \leq 0.01$), *** ($P \leq 0.001$), **** ($P \leq 0.0001$).

cant activation *via* PAC-1 and P-selectin markers even when incubated up to 20 μM (Fig. S3), indicating PolySTAT does not directly activate platelets. Although there was no measured activation, we did observe, *via* flow cytometry, that FITC-labeled PolySTAT and PolySCRAM (5 μM concentration) bound to the surface of the washed platelets (Fig. 1E). In addition, we found the binding increased in a dose dependent manner (1 μM, 5 μM, 20 μM, Fig. S4). The fibrin-binding peptide (FBP) increases the binding to platelets; further studies are necessary to understand the mechanism of platelet interaction.

PolySTAT increases clot contraction forces and the rate of force generation in human whole blood

After confirming that PolySTAT does not directly activate platelets, we measured platelet contraction forces by rheometry (Fig. 2A).[17] There has been increased interest in rheology of

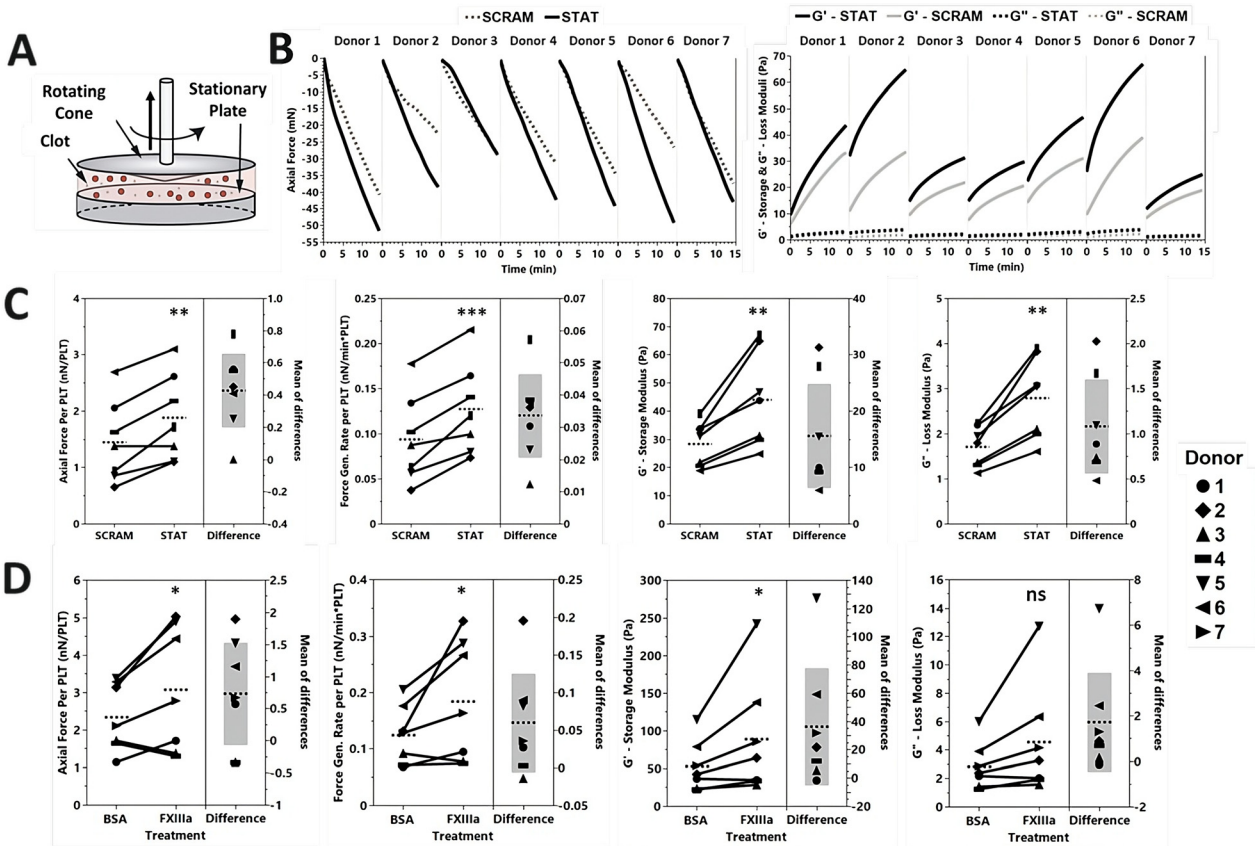

Fig. 2 PolySTAT dosed at 5 μM increases both overall clot contraction forces and the rate of force generation compared to PolySCRAM in human blood (n = 7 donors). (A) Overview of the rheological measurement of clot contraction forces. Whole blood is sandwiched between a cone and plate after being activated by thrombin. A small oscillation is applied to measure storage and loss modulus over time as the blood clots. The gap on the rheometer is fixed and the rheometer applies an upward force to maintain the gap as the blood contracts, pulling down on the cone. The force required by the rheometer to counter the platelet contraction force is reported as a negative value due to the direction it is applied on the rheometer (up = negative, down = positive). (B) Left: Axial force in mN reported for each donor, whole blood from n = 7 human donors treated with 5 μM of both PolySTAT (solid black line) and PolySCRAM (dotted light gray line). Right: Storage (G' – solid lines) and loss moduli (G'' – dotted lines) in Pa reported for each donor, PolySTAT (black) and PolySCRAM (light gray). A cubic spline fit in JMP (lambda = 0.05) was used. The negative values are due to the direction of the force on the rheometer. (C) PolySTAT showed a statistically significant increase in all measured parameters – force per platelet (left, SCRAM = 1.46 nN, STAT = 1.88 nN, mean difference = 0.43 nN, upper 95% = 0.66 nN, lower 95% = 0.20 nN, p = 0.0019), rate of force generation per platelet (center-left, SCRAM = 0.094 nN min^{-1}, STAT = 0.127 nN min^{-1}, mean difference = 0.034 nN min^{-1}, upper 95% = 0.047 nN min^{-1}, lower 95% = 0.021 nN min^{-1}, p = 0.0004), loss modulus (center-right, SCRAM = 1.71 Pa, STAT = 2.79 Pa, mean difference = 1.08 Pa, upper 95% = 1.60 Pa, lower 95% = 0.56 Pa, p = 0.0011), and storage modulus (right, SCRAM = 28.38 Pa, STAT = 44.00 Pa, mean difference = 15.62 Pa, upper 95% = 24.87 Pa, lower 95% = 6.36 Pa, p = 0.0031). (D) FXIIIa dosed at 0.1 μM increases both overall clot contraction forces and the rate of force generation compared to the BSA control in human blood (n = 7 donors). FXIIIa showed a statistically significant increase in all measured parameters except for loss modulus – force per platelet (left, BSA = 2.34 nN, FXIIIa = 3.07 nN, mean difference = 0.73 nN, upper 95% = 1.53 nN, lower 95% = −0.07 nN, p = 0.0333), rate of force generation per platelet (center-left, BSA = 0.124 nN min^{-1}, FXIIIa = 0.184 nN min^{-1}, mean difference = 0.060 nN min^{-1}, upper 95% = 0.125 nN min^{-1}, lower 95% = −0.006 nN min^{-1}, p = 0.0338), storage modulus (right-center, BSA = 53.00 Pa, FXIIIa = 89.43 Pa, mean difference = 36.43 Pa, upper 95% = 77.92 Pa, lower 95% = −5.05 Pa, p = 0.0376), and loss modulus (right, BSA = 2.84 Pa, FXIIIa = 4.56 Pa, mean difference = 1.72 Pa, upper 95% = 3.91 Pa, lower 95% = 0.47 Pa, p = 0.0514). A linear fit was done to the linear portions of the axial stress *vs.* time data and the slope was taken as the rate of force generation. A matched pairs one-sided t-test (α = 0.050) was used to compare treatments. The following significance labels were used: ns (P > 0.05), * ($P \leq 0.05$), ** ($P \leq 0.01$), *** ($P \leq 0.001$), **** ($P \leq 0.0001$).

human blood work recently.[18–20] We used a cone and plate rheometer with a small blood volume and sandblasted surfaces to prevent clot retraction. In this system, as the blood clots, platelets begin to pull down on the cone, and the rheometer applies a normal force to counteract the platelet contraction forces to maintain a constant gap height. At the same time, the clots are subjected to a small amplitude oscillatory strain (SAOS) of 3% to measure bulk mechanical properties of the clots. The spline averages of n = 3 runs per treatment (PolySTAT or PolySCRAM dosed at 5 μM) for each of the n = 7 human donors measured are shown in Fig. 2B. We observed a consistent, statistically significant trend where PolySTAT-treated clots not only achieved higher axial stress values, but also a faster rate of force generation (Fig. 2C). Platelet counts were comparable across donors. Therefore we directly normalized by donor platelet count and found that PolySTAT-treated blood resulted in a ∼29% increase (upper 95% = ∼45%, lower 95% = ∼14%) in the amount of force generated per platelet, and ∼36% increase (upper 95% = ∼50%, lower 95% = ∼22%) in the rate of force generation per platelet. Tutwiler *et al.* found that clot contraction can be broken down into three phases: (1) initiation, where platelets are activating, the fibrin network is forming, and platelets are binding fibrinogen/fibrin; (2) linear, where platelets are contracting, the fibrin network is remodeling, and fibrin is starting to be crosslinked by factor XIIIa (FXIIIa); and (3) mechanical clot stabilization driven by FXIIIa. When FXIIIa is inhibited, clot contraction stalls and cannot undergo phase 3 (clot stabilization), which is the phase when the most contraction occurs.[11] FXIIIa is a transglutaminase that creates permanent γ-glutamyl-ε-lysinyl isopeptide bonds, chemically crosslinking together the γ- and α-chains of fibrin.[21] PolySTAT similarly crosslinks fibrin by non-covalently bridging DDE regions, but its bonds are reversible. Because both create intra- and inter-protofibril crosslinks, we were interested to see if FXIIIa, like PolySTAT, would increase platelet contraction forces. Indeed, a 0.1 μM addition of FXIIIa to human blood resulted in similar trends to PolySTAT treated clots, including higher axial stress values, and increased the rate of force generation (Fig. S5). Similar to PolySTAT, we observed ∼31% increase (upper 95% = ∼65%, lower 95% = ∼−3%) in the amount of force generated per platelet, and ∼48% increase (upper 95% = ∼101%, lower 95% = ∼−5%) in the rate of force generation per platelet compared to the BSA negative control.

PolySTAT prevents inter-protofibril sliding and helps restore intra-protofibril knob-hole connections after yielding

To understand how PolySTAT's impact on the fibrin network might affect conduction of platelet contractile forces, we conducted Large Amplitude Oscillatory Shear (LAOS) testing in a purified fibrinogen and thrombin system. Small Amplitude Oscillatory Shear (SAOS) testing only evaluates the linear viscoelastic range. It is well-characterized in the literature that fibrin networks only exhibit linear viscoelastic properties in very small strain amplitudes (<5% strain amplitude).[22–26] In this range, rheological measurements are only evaluating bulk mechanical properties of fibrin gels and stressing large fibrin fibrils, with purely elastic deformation. Physiologically the linear viscoelastic range is akin to a resting clot. By increasing the % strain amplitude (>5%), we can probe the nonlinear viscoelastic range and evaluate the microstructure of fibrin – moving from inter-protofibril sliding (∼10% strain amplitude) to intra-protofibril sliding (∼100% strain amplitude) until failure of the fibrin network occurs (Fig. 3A). Physiologically, the non-linear viscoelastic range reflects stresses from blood flow and platelet contraction consistent with those found in trauma settings. LAOS testing, coupled with the Series of Physical Processes (SPP) framework, provides a powerful approach for characterizing this nonlinear behavior with the addition of a physical interpretation of the thixotropic or time-dependent rheological properties.[27–29] Since PolySTAT-mediated strengthening early in coagulation appeared to be key, we used LAOS to investigate the fibrin network directly.

In the purified fibrinogen system, we found that PolySTAT clots consistently produced larger storage moduli than the control clots, becoming statistically significant in the non-linear viscoelastic range (10% strain amplitude) (Fig. 3B).[24] For all the treatments, there was an increase in storage modulus with increasing strain confirming the well-documented strain-stiffening property of fibrin clots.[24,25,30] This strain-stiffening behavior also occurs intracycle at each strain amplitude as evidenced by the Cole–Cole plots (Fig. S6–S8). At 100% strain amplitude, the peak storage modulus is highest in the PolySTAT clots 2.78 (Pa) compared to the negative control 1.71 (Pa) ($p \leq 0.05$), and PolySCRAM 1.39 (Pa) (p = 0.01). The increase in clot stiffness reflects reduced inter-protofibril sliding, indicating that PolySTAT reinforces the domains that span neighboring protofibrils, resulting in more elastic clots. Similarly, Martinez-Torres *et al.* found that FXIIIa crosslinking prevented inter-protofibril sliding, significantly affecting fibrin network mechanics under LAOS.[31] PolySTAT clots are therefore more resistant to deformation and tend to return to their original shape after stress is removed better than the control clots. While PolySTAT clots demonstrate a higher peak storage modulus compared to controls, PolySTAT clots also exhibit a statistically-higher viscous modulus than the control clots both in the linear and nonlinear viscoelastic range (Fig. 4C), suggesting that PolySTAT clots dissipate more energy than the other clots when subjected to deformation.

Therefore, PolySTAT-treated clots display a unique balance where they are not only stiffer, but they also accommodate deformation without immediate failure, suggesting that PolySTAT clots have a more adaptable network structure. To further investigate yielding of the network, the Phase Angle Velocity (PAV) was plotted as a function of strain. Donley *et al.* showed the PAV allows for the quantitative analysis of yielding (positive PAV) and reforming (negative PAV) of a material's microstructure for LAOS data.[29] PAV is a unique metric that the SPP framework enables with its instantaneous calculation of viscoelastic moduli (Fig. S9). At the peak 100% strain amplitude, there is no statistical difference in the yielding metric between the three clot types (Fig. 3C), which is to be expected

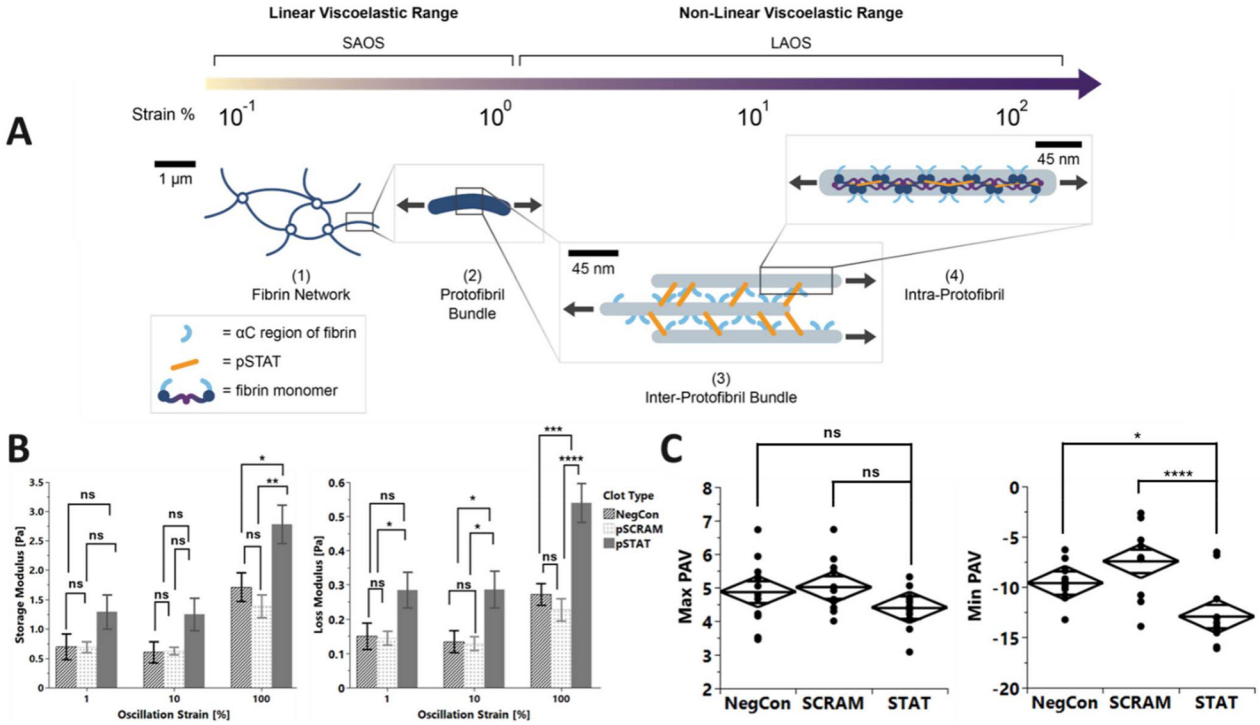

Fig. 3 Large Amplitude Oscillatory Shear (LAOS) of purified fibrinogen clots. (A) Overview of percent strain amplitude applied during SAOS and LAOS, along with corresponding microstructural changes measured with increasing percent strain amplitude. 1. Network made up of protofibril bundles – initial stiffness due to thermal fluctuations. 2. Protofibril bundle slack removal resulting in first strain stiffening behavior (avg. diameter ranges between 80–500 nm). 3. Inter-protofibril bundle sliding leading to eventual failure in strain regimes beyond 100%. 4. Intra-protofibril sliding during protofibril stretching. Eventually, reforming of intra-protofibril bonds lead to 2nd strain stiffening behavior. Created by Dr Lucy F. Yang. (B) Storage modulus (left, [all data reported as mean, upper 95%, lower 95%] PSTAT = 1.29 Pa, 1.25 Pa, 2.78 Pa; PSCRAM = 0.69 Pa, 0.62 Pa, 1.39 Pa; negative control = 0.70 Pa, 0.61 Pa, 1.71 Pa) as a function of strain amplitude in purified fibrin clots. Loss modulus (right, [all data reported as mean, upper 95%, lower 95%] PSTAT = 0.285 Pa, 0.286 Pa, 0.540 Pa; PSCRAM = 0.144 Pa, 0.128 Pa, 0.227 Pa; negative control = 0.150 Pa, 0.135 Pa, 0.272 Pa) as a function of strain amplitude in purified Fibrinogen clots. (C) Phase Angle Velocity (PAV), metric of yielding (positive) and reforming (negative), at 100% strain amplitude PSTAT = −12.9, PSCRAM = −7.42, negative control = −9.58. Equations located in SI. There was no statistical significance between positive (yielding) values. Each treatment had a sample size of n = 12. A fit model for a repeated measure, one-way Anova with Tukey *post-hoc* analysis (α = 0.050) was used to compare treatments. The following significance labels were used: ns ($P > 0.05$), * ($P \leq 0.05$), ** ($P \leq 0.01$), *** ($P \leq 0.001$), **** ($P \leq 0.0001$).

as the yield point of fibrin occurs at a higher strain amplitude beyond the capability of our instrument. The reforming metric does show a statistically significant difference, however, with PolySTAT showing a time-normalized Phase Angle Velocity of −12.9, PolySCRAM −7.4 (p = 0.0001), and negative control −9.58 (p = 0.019) (Fig. 3C). The larger the magnitude of the negative PAV the greater the extent to which the material is undergoing restructuring and reforming of the microstructure. Quantitatively PolySTAT-treated clots undergo microstructure reforming that is 43% greater than PolySCRAM and 26% greater than control clots. Microstructurally, this means that PolySTAT is enhancing the ability of the inter-protofibril connections in fibrin to reform after yielding.

Fig. 4 summarizes the proposed microstructural reinforcement by PolySTAT measured by LAOS. PolySTAT bridges both intra- and inter-protofibril binding between αC domains (inter-protofibril) and the A-knob/A-hole & B-knob/B-hole interactions (intra-protofibril) (Fig. 4A and B). These interactions occur in the combined D-domains and E domain referred to as the "DDE sections" of fibrin protofibrils. This physical crosslinking enables the network to distribute stress more efficiently by preventing inter-protofibril sliding (Fig. 4C), increasing the capacity of the network to dissipate strain through viscous interactions and the rate of reforming of DDE section interactions (Fig. 4D). These microstructural enhancements to fibrin by PolySTAT create stronger clots that better endure plastic deformation than the control clots and reform to a greater extent after yielding during platelet-induced clot contraction. We hypothesize these changes to the mechanical properties of fibrin would result in a stiffer fibrin substrate that would both endure greater contraction forces from the mechanosensing platelets and more efficiently translate platelet contraction forces across the fibrin network.

We hypothesize that these changes in fibrin mechanics would produce a stiffer substrate and more efficiently transmit forces across the network, thereby amplifying platelet-driven contraction. *In vivo*, fibrin clots experience dynamic forces, such as high shear stress from rapid blood flow and disturbed

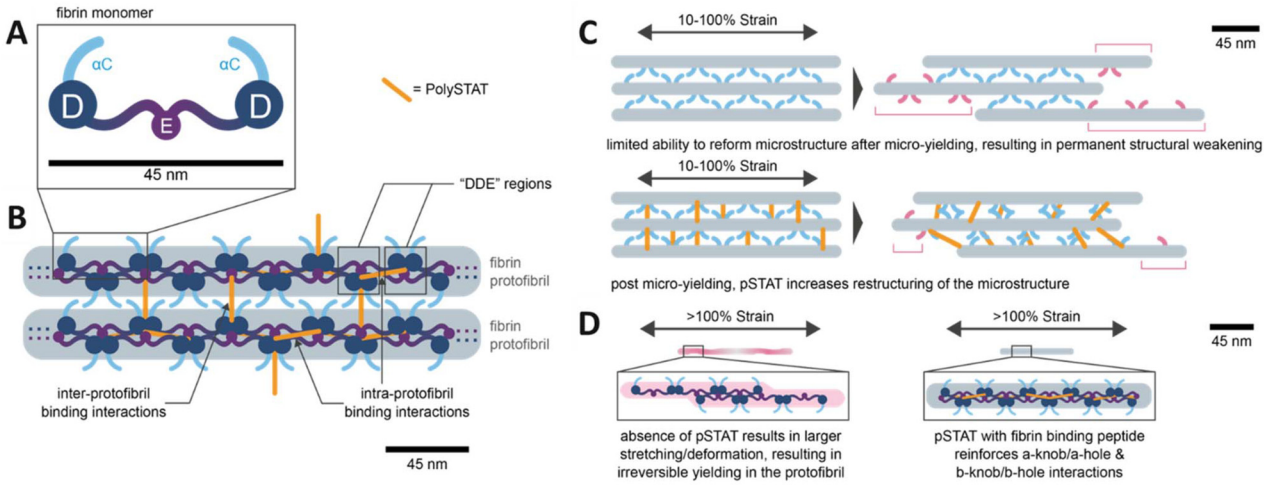

Fig. 4 Overview of PolySTAT reinforcement leading to measured differences in LAOS. (A) Fibrin monomer with its D, E, and αC Regions identified. (B) PolySTAT is hypothesized to bridge DDE sections (DDE section refers to the binding domains of a fibrin monomer which contains a middle E-domain and two outer D-domains) both intra and inter (crossing alpha C regions) fibrin protofibrils. (C) The inter-protofibril reinforcement strengthens the αC regions and prevents protofibril sliding, while also increasing the rate of protofibril restructuring. (D) The intra-protofibril reinforcement increases the rate of reforming protofibrils after the fibrils yield during shear at strain amplitudes 100%. This is reflected in the minimum PAV. Figure created by Dr Lucy F. Yang.

vessel geometry. PolySTAT enhances clot contraction, increasing fibrin stiffness and force transmission (Fig. 2 and 3), which may expedite wound closure and limit blood loss. In rat trauma models, PolySTAT improved survival and reduced bleeding without evidence of embolism or premature clot failure, though excessive early contraction could pose risks under high shear. Further *in vivo* studies are needed to confirm PolySTAT's stability and safety in dynamic vascular settings.

3. Experimental

Materials

Human whole blood was purchased from Bloodworks Northwest (Seattle, WA). 2,2′-azobis(2-methylpropionitrile) (AIBN), 4-((((2-carboxyethyl)thio)carbonothioyl)thio)-4-cyanopentanoic acid (CCC), glycidyl methacrylate (GMA), anhydrous *N*,*N*-dimethylacetamide (DMAc), anhydrous dimethyl sulfoxide (DMSO), diethyl ether, acetone, (±)-1-amino-2-propanol, bovine serum albumin (BSA), and all other reagents were purchased from Sigma-Aldrich (Saint Louis, MO) unless noted otherwise. *N*-Hydroxysuccinimide methacrylate (NHSMA) was purchased from TCI America (Portland, OR). The fibrin-binding peptide (FBP; sequence: Ac-Tyr-{D-Glu}-Cys-Hyp-{Tyr(3-Cl)}-Gly-Leu-Cys-Tyr-Ile-Gln-Gly-Lys-NH2),[32] developed by the Caravan group, and the scrambled peptide (SCRAM; sequence: Ac-Tyr-Ile-Cys-Gly-Gln-{D-Glu}-Ala-Cys-Hyp-Leu-Tyr-Gly-Lys-NH2) were both purchased from CPC Scientific (San Jose, California) as custom orders. All purified clotting factors – human fibrinogen, plasminogen depleted (FIB 1), human alpha-thrombin (HT 1002a), human plasmin (HPlasmin), and human FXIIIa (HFXIIIa 1314) were purchased from Enzyme Research Laboratories (South Bend, IN). EXTEM and APTEM reagents for the ROTEM Delta were purchased from Werfen (Bedford, MA).

Synthesis of PolySTAT *via* conjugation

PolySTAT and PolySCRAM used in these studies were synthesized *via* the post-polymerization peptide conjugation method previously reported.[10] Multiple batches of PolySTAT and PolySCRAM were used. All treatments in these studies used the glycerol monomethacrylate (GmMA) backbone. Table S1 gives an overview of the range of degrees of polymerization (DP), molecular weights (MW), and peptides per polymer for the PolySTAT and PolySCRAM used in these studies.

Hydrolysis of glycidyl methacrylate to glycerol monomethacrylate

Briefly, glycerol monomethacrylate (GmMA) was synthesized *via* hydrolysis of glycidyl methacrylate (GMA) as described previously.[10] GMA (11.4 mL) was added to deionized (DI) water (68.6 mL) at a mass ratio of 15% in a two-necked round bottom flask (RBF) with one neck sealed and a Vigreux column in the other. The mixture was sparged with air and stirred at 80 °C for 16 h. The solution was subsequently cooled, and sodium chloride added to a final concentration of 300 mg mL^{-1}. GmMA was extracted into an organic phase *via* 3× washes with 30 mL ethyl acetate. GmMA was isolated by removal of ethyl acetate *via* rotovap and stored at −20 °C.

Synthesis of p(GmMA-*co*-NHSMA) statistical copolymer

The statistical copolymer backbone p(GmMA-*co*-NHSMA) was synthesized *via* reversible addition–fragmentation chain trans-

fer (RAFT) polymerization as described previously.[10] Briefly, GmMA was combined with NHSMA, CCC, and AIBN at 160 : 40 : 1 : 0.2 ratio, respectively, in dimethylacetamide at a monomer concentration of 0.6 M in a round bottom flask (RBF). This mixture reacted for 14 h at 70 °C. P(GmMA-*co*-NHSMA) copolymers were precipitated in diethyl ether followed by dissolution in dimethyl sulfoxide (DMSO) and a second precipitation in 50–50 acetone/diethyl ether. Precipitated polymer was collected by centrifugation at 7197*g*. Trithiocarbonate groups were removed *via* an end-capping reaction with 20× molar excess AIBN at 70 °C for 12 hours.

Peptide Conjugation

FBP was conjugated to the p(GmMA-*co*-NHSMA) synthesized above *via* reaction of the C-terminal lysine in FBP as previously described.[10] Briefly, p(GmMA-*co*-NHSMA) was dissolved at 50 mg mL^{-1} in anhydrous DMSO in an RBF. FBP was then added at a ratio of 0.4 : 1 peptide to NHSMA. *N*,*N*-Diisopropylethylamine was then added at a 5 : 1 ratio base : peptide, and the RBF was sealed, and the reaction was stirred for 24 h at 50 °C, after which unreacted NHSMA groups were capped with 10× molar ratio of 1-amino-2-propanol (A2P). Peptide-polymer conjugates were purified by extensive dialysis as follows. First, the product was dialyzed against DMSO for 24 h (1 bath change, 1 L bath). Next, the polymer was moved to phosphate-buffered saline (PBS) for 24 h (3 buffer changes, 4 L bath) during which a precipitate formed. The contents of the dialysis bag were collected and centrifuged at 4127*g* for 30 min to remove insoluble material; the supernatant was collected and moved to a fresh dialysis bag. Dialysis was continued in DI H_2O for 48 h (6 bath changes, 4 L bath) to remove PBS salts. The contents of the dialysis bag were collected and centrifuged at 4127*g* for 30 min to remove insoluble material. Then the supernatant was 0.2 μm sterile filtered into a 50 mL conical Falcon tube, flash frozen in liquid nitrogen, and lyophilized for 3 days.

PolySTAT characterization

All PolySTAT and PolySCRAM batches were characterized for QC as previously reported.[10,33] Briefly, backbone polymers were characterized *via* GPC in dimethylformamide with static light scattering and refractive index detectors (MiniDawn Treos and OptilabTRex, respectively, both from Wyatt Technology, Santa Barbara, CA) to determine molecular weight and dispersity index (PDI). ^{1}H nuclear magnetic resonance (NMR) spectroscopy on a Bruker AV 300 was utilized to determine conversion of the polymer prior to purification, and composition after purification. ROTEM whole blood hemostasis analyzer (ROTEM, Instrumentation Laboratory, Bedford, MA, USA) was used to confirm activity of different PolySTAT formulations under hyperfibrinolysis conditions in a purified human fibrinogen system. 300 μL of a clotting solution with final concentrations in the ROTEM were 1.5 mg mL^{-1} fibrinogen, 1 IU mL^{-1} thrombin, 1–4 μg mL^{-1} plasmin, 0.1 mmol L^{-1} $CaCl_2$, and 5 μmol L^{-1} PolySTAT at pH 7.4.

Rotational thromboelastometry (ROTEM) evaluation

Animal experiments were conducted in accordance with guidelines from the University of Washington that are based on the National Research Council's Guide for the Care and Use of Laboratory animals, and all protocols were approved by the University of Washington Institutional Care and Use Committee. PolySTAT was dosed at 5 μM, a concentration efficacious and safe in previous preclinical TEG, ROTEM, and rat testing of PolySTAT.[10] This concentration would be a clinically achievable plasma level *via* intravenous (IV) administration. Whole blood from rat and swine were collected during severe hemorrhage trauma models. Whole human blood was purchased from Bloodworks Northwest (50 mL total blood in 3.2% sodium citrate). Two ROTEM deltas (Werfen, Bedford, MA/Serial #s 3733 and 4515) were used using the standard manufacturer's protocol for Extrinsic Thromboelastometry or EXTEM ($CaCl_2$ + recombinant tissue factor + polybrene) and Aprotinin-containing Thromboelastometry or APTEM ($CaCl_2$ + recombinant tissue factor + polybrene + aprotinin) for both whole blood and platelet poor plasma (PPP, centrifuged 1500*g* for 15 minutes). For each test, 15 μL of a treatment stock solution (100 μM) was pipetted directly into the ROTEM cup followed by the standard ROTEM automatic pipetting sequence of reagents (EXTEM or APTEM) and 300 μL of whole blood or PPP.

Rheometer measurement of clot contraction forces

A method based on Tutwiler *et al.* was used to measure clot contraction forces.[34] Healthy donor whole blood was collected in standard 3.2% sodium citrate tubes (n = 3 tubes per donor). The blood was evaluated within 4 hours of the blood draw, and all citrated tubes were combined in a 15 mL Falcon tube to eliminate tube to tube variability. A TA Instruments Discovery Series Hybrid Rheometer (DHR-3) equipped with a solvent trap was used to measure the normal axial forces required to maintain a fixed gap height in response to clot contraction. All experiments were conducted at 37 °C, 3% strain, 5 rad s^{-1} with a 20 mm sandblasted, stainless steel cone and plate (1 degree). A rheometer gap of 313 μm with 131.75 μL of blood was used. Samples were reconstituted by combining the following in the order written: 7.75 μL of treatment (PolySTAT/PolySCRAM [Final Conc. 5 μM], FXIIIa/BSA [Final Conc. 30 μg mL^{-1}]), 7.75 μL of thrombin [Final Conc. 1 IU mL^{-1}], 7.75 μL $CaCl_2$ solution [Final Conc. 10 mM], and 131.75 μL of citrated blood in a 1.5 mL Eppendorf tube. The contents were mixed by gently pipetting up and down 6× using a P200 pipette and immediately 131.75 μL of the activated blood was pipetted onto the Peltier plate of the rheometer. Quickly, the gap was set, and the normal force was zeroed, prior to initiating the run. All N = 3 repeats for each treatment condition were completed for each donor. Due to the shelf-life of the platelets in the blood (4 hours), and time for sample preparation and testing (~25 min per run), only two treatment conditions could be compared per donor in order to complete N = 3 repeats per treatment (total of 6 runs per donor).

Platelet activation assay with PolySTAT

Aliquots of whole blood (450 μL) were incubated for 5 min at room temperature with 50 μL of 50 μM polySTAT or polySCRAM (using a scrambled peptide version as a nonfunctional control), DPBS 2% fetal bovine serum (FBS, Gibco), or adenosine diphosphate (ADP, Bio/Data) for positive activation control. Aliquots (5 μL) were incubated with antibody solutions of FITC antihuman PAC-1 (1 : 10, BD Biosciences), APC antihuman CD62P (1 : 10, BD Biosciences), and/or PE antihuman CD61 (1 : 10, BD Biosciences) for 20 min at room temperature. Cells were fixed in DPBS 1% PFA and analyzed on an Attune NxT (Invitrogen) flow cytometer.

PolySTAT binding assay

Whole blood (Bloodworks) was centrifuged at 200*g* for 20 min at room temperature. Platelet-rich plasma from the top layer was diluted at 1 : 1 v/v ratio with Dulbecco's phosphate-buffered saline (DPBS, Gibco) supplemented with 2 mM ethylenediaminetetraacetic acid (EDTA, Invitrogen) and centrifuged at 100*g* for 20 min at room temperature. The supernatant was separated and centrifuged at 800*g* for 20 min at room temperature to pellet platelets. Platelets were rinsed with DPBS 2 mM EDTA and resuspended in DPBS. Aliquots of 10^6 platelets were pelleted at 800*g* for 5 min at room temperature and incubated for 20 min at room temperature with 20, 5, 1, or 0 μM of FITC-labelled polySTAT or polySCRAM in DPBS supplemented with 1% bovine serum albumin (Miltenyi). Platelets were fixed in 200 μL of DPBS 1% BSA 0.1% paraformaldehyde (Alfa Aesar) and analyzed on an Attune NxT (Invitrogen) flow cytometer.

Large amplitude oscillatory shear (LAOS) probing

Clots were prepared from human alpha thrombin and fibrinogen solutions depleted of plasminogen and vWF purchased from Enzyme Research Laboratories (South Bend, IN). Three clot types were prepared: a negative control with no polymer added, one with a PolySCRAM and one with PolySTAT. Total volume of each clot was approximately 440 μL with final concentrations of fibrinogen (2 mg ml^{-1}), thrombin (1 IU ml^{-1}), $CaCl_2$ (10 mM), and polymer (5 μM). The clots were mixed by pipetting six times in a 2 mL Eppendorf tube immediately prior to depositing on the rheometer. The fibrinogen and thrombin were kept separated until immediately prior to mixing and testing. Thrombin was diluted in HEPES on ice and fibrinogen diluted in HEPES at 37 °C. A sandblasted, 40 mm parallel plate geometry was attached to a DHR-3 rheometer with the TRIOS software, gap height 300 μm, and temperature 37.0 °C (controlled by Peltier plate). Oscillatory Strain Amplitude sweep was run from 0.01 [–] to 100.0 [–] at a frequency of 0.1 Hz with two cycles conditioning time and one cycle sampling time. The large strain amplitude range was necessary due to significant differences between linear and non-linear viscoelastic behavior of clots as well as the physiologically relevant strain regime present in most trauma models.[24] LAOS data was processed through the Series of Physical Processes (SPP) framework from the Rogers group according to published methods.[27–29] SPP allows for intracycle thixotropic analysis of LAOS data. The non-linear viscoelastic data is both physiologically relevant as well as necessary to determine the microstructural differences between polySTAT treated clots and control clots.[35–37]

4. Conclusions

Platelet-induced clot contraction is a crucial step in hemostasis and wound-healing that minimizes blood loss. We observed that our polymeric hemostat, PolySTAT, which physically crosslinks fibrin through non-covalent binding interactions, induces more clot contraction compared to control clots. In this work, we evaluated mechanisms for PolySTAT-associated clot contraction. We first quantified contraction forces and showed that PolySTAT increased (1) the rate of platelet contraction forces, (2) overall clot contraction forces, and (3) the storage modulus of whole blood clots in normal human blood. Addition of the natural fibrin crosslinking enzyme FXIIIa, early in the clotting process recapitulates these PolySTAT-associated changes, suggesting that PolySTAT's fibrin crosslinking ability is responsible for the observed effects on clot contraction. We further confirmed that PolySTAT's enhancement of clot contraction is an indirect property independent of platelet activation. Using rheology and LAOS analysis, we demonstrated that the likely mechanism is a PolySTAT-induced increase of the mechanical transduction efficiency of the fibrin network early on in clotting, enabling clot contraction to occur faster and by providing a stiffer fibrin substrate inducing platelets to contract more forcefully. Enhanced clot contraction from synthetic hemostats has also been observed by the Brown group, who reported that their platelet-like particles enhance clot contraction through a Brownian ratchet mechanism, increasing clot density and stability within a 24-hour time period.[38–41] To our knowledge, PolySTAT is the first synthetic hemostatic agent that rapidly facilitates clot contraction within minutes of exposure to forming clots. While clot contraction expediates wound closure, we have not yet demonstrated the effect of PolySTAT-induced clot contraction on survival after trauma. The contraction of clots is essential and beneficial to hemostasis and wound healing; however, over contraction of clots early on in coagulation might cause early clot disruption rather than strengthening. *In vivo*, fibrin clots are exposed to dynamic mechanical forces, especially in trauma settings where rapid blood flow and disrupted vessel geometry generate high shear stress and strain.[42,43] Further studies are needed to understand the *in vivo* effects of PolySTAT-enhanced clot contraction.

Author contributions

T. J. P. and T. C.: conceptualized the manuscript, designed the rheological experiments, synthesized and characterized

PolySTAT/PolySCRAM, analyzed results, and prepared the manuscript; M. L., M. D., and A. T.: completed platelet studies and analyzed results; A. T., M. B., M. H., and D. F. analyzed results and helped investigate the ROTEM results; M. A.: consulted and analyzed LAOS results; S. H. P. and N. J. W.: acquired funding in support of the work; all authors reviewed and edited the manuscript.

Conflicts of interest

There are no conflicts to declare.

Data availability

Data for this article is available at Mendeley Data, V1, **https://doi.org/10.17632/27knvfh68s.1**.

Supplementary information (SI) is available. See DOI: **https://doi.org/10.1039/d5bm01101a**.

Acknowledgements

We thank Dr Lucy F. Yang (Scientific Figure Consultant) for her assistance in creating Fig. 3A and 4. This work was supported by NIH NHLBI (1R01HL139007) and NIH NIBIB (1R01EB036076). T. J. P. was supported by a National Science Foundation Graduate Research Fellowship under grant no. DGE-1762114. M. L. was also supported by a National Science Foundation Graduate Research Fellowship under grant no. DGE-214004. T. C. was supported and funded by the U.S. Army, and the Department of Chemistry and Life Science, United States Military Academy at West Point. The views expressed herein are those of the authors and do not reflect the position of the United States Military Academy, the Department of the Army, or the Department of Defense. LAOS data was analyzed with the Series of Physical Processes Framework generously shared by Professor Simon Rogers of the Simon Rogers Group for Soft Matter Research out of The University of Illinois at Urbana-Champaign.

References

1 N. D. Rossiter, *Int. Orthop.*, 2022, **46**, 3–11.
2 T. Vos, *et al.*, *Lancet*, 2020, **396**, 1204–1222.
3 T. J. Pichon, N. J. White and S. H. Pun, *Curr. Opin. Biomed. Eng.*, 2023, **27**, 100456.
4 G. McGwin, A. M. Nunn, J. C. Mann, R. Griffin, G. G. Davis, P. A. MacLennan, J. D. Kerby, J. E. Acker and L. W. Rue, *J. Trauma:Inj., Infect., Crit. Care*, 2009, **66**, 526–530.
5 J. A. Evans, K. J. P. Van Wessem, D. McDougall, K. A. Lee, T. Lyons and Z. J. Balogh, *World J. Surg.*, 2010, **34**, 158–163.
6 B. Mitra, F. Tullio, P. A. Cameron and M. Fitzgerald, *Emerg. Med. J.*, 2012, **29**, 622–625.
7 J. O. Barbosa Neto, M. F. B. de Moraes, R. S. Nani, J. A. Rocha Filho and M. J. C. Carmona, *Rev. Bras. Anestesiol.*, 2013, **63**, 103–106.
8 R. J. Ramirez, P. C. Spinella, G. V. Bochicchio and L. M. Napolitano, *Tranexamic Acid Update in Trauma*, 2016.
9 L. W. Chan, X. Wang, H. Wei, L. D. Pozzo, N. J. White and S. H. Pun, *Sci. Transl. Med.*, 2015, **7**, 277ra29.
10 R. J. Lamm, T. J. Pichon, F. Huyan, X. Wang, A. N. Prossnitz, K. T. Manner, N. J. White and S. H. Pun, *ACS Biomater. Sci. Eng.*, 2020, **6**, 7011–7020.
11 R. J. Lamm, E. B. Lim, K. M. Weigandt, L. D. Pozzo, N. J. White and S. H. Pun, *Biomaterials*, 2017, **132**, 96–104.
12 W. A. Lam, O. Chaudhuri, A. Crow, K. D. Webster, T.-D. Li, A. Kita, J. Huang and D. A. Fletcher, *Nat. Mater.*, 2011, **10**, 61–66.
13 O. Oshinowo, S. S. Azer, J. Lin and W. A. Lam, *J. Thromb. Haemostasis*, 2023, **21**, 2339–2353.
14 S. E. Dekker, V. A. Viersen, A. Duvekot, M. de Jong, C. E. van den Brom, P. M. van de Ven, P. Schober and C. Boer, *Anesthesiology*, 2013, **63**, 103–106.
15 N. Katori, K. A. Tanaka, F. Szlam and J. H. Levy, *Anesth. Analg.*, 2005, 1781–1785.
16 E. E. Jansen and M. Hartmann, *Biomedicines*, 2021, **9**, 1064.
17 V. Tutwiler, H. Wang, R. I. Litvinov, J. W. Weisel and V. B. Shenoy, *Biophys. J.*, 2017, **112**, 714–723.
18 M. Armstrong, M. Scully, M. Clark, T. Corrigan and C. James, *J. Non-Newtonian Fluid Mech.*, 2021, **290**, 104503.
19 T. Corrigan, L. O'Malley, D. Bailey, H. Moseley, J. Okaikoi, T. Brown, S. Murray, W. Chang, M. Yang, L. Nguyen, E. Milner, K. O'Donovan and M. Armstrong, *Open J. Fluid Dyn.*, 2021, **11**, 167–176.
20 M. Armstrong, K. Rook, W. Pulles, M. Deegan and T. Corrigan, *Rheol. Acta*, 2021, **60**, 119–140.
21 R. A. S. Ariëns, T.-S. Lai, J. W. Weisel, C. S. Greenberg and P. J. Grant, *Blood*, 2002, **100**, 743–754.
22 J. V. Shah and P. A. Janmey, *Rheol. Acta*, 1997, **36**, 262–268.
23 U. Windberger and J. Läuger, *Molecules*, 2020, **25**, 3890.
24 K. M. Weigandt, N. White, D. Chung, E. Ellingson, Y. Wang, X. Fu and D. C. Pozzo, *Biophys. J.*, 2012, **103**, 2399–2407.
25 E. A. Ryan, L. F. Mockros, J. W. Weisel and L. Lorand, *Biophys. J.*, 1999, **77**, 2813–2826.
26 T. F. Lamer, B. R. Thomas, D. J. Curtis, N. Badiei, P. R. Williams and K. Hawkins, *Phys. Fluids*, 2017, **29**, 121606.
27 S. Rogers, *Phys. Today*, 2018, **71**, 34–40.
28 S. A. Rogers, B. M. Erwin, D. Vlassopoulos and M. Cloitre, *J. Rheol.*, 2011, **55**, 435–458.
29 G. J. Donley, J. R. de Bruyn, G. H. McKinley and S. A. Rogers, *J. Non-Newtonian Fluid Mech.*, 2019, **264**, 117–134.
30 I. K. Piechocka, R. G. Bacabac, M. Potters, F. C. MacKintosh and G. H. Koenderink, *Biophys. J.*, 2010, **98**, 2281–2289.
31 C. Martinez-Torres, J. Grimbergen, J. Koopman and G. H. Koenderink, *J. Thromb. Haemostasis*, 2024, **22**, 715–726.
32 A. F. Kolodziej, S. A. Nair, P. Graham, T. J. McMurry, R. C. Ladner, C. Wescott, D. J. Sexton and P. Caravan, *Bioconjugate Chem.*, 2012, **23**, 548–556.

33 C. M. Heinze, T. J. Pichon, A. Y. Wu, M. Baldwin, J. Matthaei, K. Song, M. Sylvestre, J. Gustafson, N. J. White and M. C. Jensen, *J. Am. Chem. Soc.*, 2025, **147**, 5149–5161.
34 V. Tutwiler, R. I. Litvinov, A. P. Lozhkin, A. D. Peshkova, T. Lebedeva, F. I. Ataullakhanov, K. L. Spiller, D. B. Cines and J. W. Weisel, *Blood*, 2016, **127**, 149–159.
35 R. H. Ewoldt, *J. Rheol.*, 2013, **57**, 177–195.
36 R. H. Ewoldt, A. E. Hosoi and G. H. McKinley, *J. Rheol.*, 2008, **52**, 1427–1458.
37 K. Hyun, M. Wilhelm, C. O. Klein, K. S. Cho, J. G. Nam, K. H. Ahn, S. J. Lee, R. H. Ewoldt and G. H. McKinley, *Prog. Polym. Sci.*, 2011, **36**, 1697–1753.
38 S. Nandi, E. P. Sproul, K. Nellenbach, M. Erb, L. Gaffney, D. O. Freytes and A. C. Brown, *Biomater. Sci.*, 2019, **7**, 669–682.
39 A. C. Brown, S. E. Stabenfeldt, B. Ahn, R. T. Hannan, K. S. Dhada, E. S. Herman, V. Stefanelli, N. Guzzetta, A. Alexeev, W. A. Lam, L. A. Lyon and T. H. Barker, *Nat. Mater.*, 2014, **13**, 1108–1114.
40 Y. Qiu, A. C. Brown, D. R. Myers, Y. Sakurai, R. G. Mannino, R. Tran, B. Ahn, E. T. Hardy, M. F. Kee, S. Kumar, G. Bao, T. H. Barker and W. A. Lam, *Proc. Natl. Acad. Sci. U. S. A.*, 2014, **111**, 14430–14435.
41 A. R. Wufsus, K. Rana, A. Brown, J. R. Dorgan, M. W. Liberatore and K. B. Neeves, *Biophys. J.*, 2015, **108**, 173–183.
42 D. L. Bark and D. N. Ku, *J. Biomech.*, 2010, **43**, 2970–2977.
43 G. J. Tangelder, D. W. Slaaf, T. Arts and R. S. Reneman, *Am. J. Physiol.: Heart Circ. Physiol.*, 1988, **254**, H1059–H1064.